




Review

Polypyrrole-Based Metal Nanocomposite Electrode Materials for High-Performance Supercapacitors [†]

Ganesh Shimoga ^{1,*}, Ramasubba Reddy Palem ^{2,†}, Dong-Soo Choi ³ , Eun-Jae Shin ¹, Pattan-Siddappa Ganesh ¹, Ganesh Dattatraya Saratale ⁴ , Rijuta Ganesh Saratale ⁵, Soo-Hong Lee ² and Sang-Youn Kim ^{1,*} 

¹ Interaction Laboratory, Future Convergence Engineering, Advanced Technology Research Center, Korea University of Technology and Education, Cheonan-si 31253, Korea; ejshin@koreatech.ac.kr (E.-J.S.); ganeshps11@gmail.com (P.-S.G.)

² Department of Medical Biotechnology, Dongguk University Biomedical, Campus 32, Seoul 10326, Korea; palemsubbareddy@gmail.com (R.R.P.); soohong@dongguk.edu (S.-H.L.)

³ School of Computer Science, College of Engineering and Information Technology, Semyung University, Jecheon 27136, Korea; dschoi@semyung.ac.kr

⁴ Department of Food Science and Biotechnology, Dongguk University-Seoul, Ilsandong-gu, Goyang-si, Seoul 10326, Korea; gdsaratale@gmail.com

⁵ Research Institute of Biotechnology and Medical Converged Science, Dongguk University-Seoul, Ilsandong-gu, Goyang-si, Seoul 10326, Korea; rijutaganesh@gmail.com

* Correspondence: shimoga@koreatech.ac.kr (G.S.); sykim@koreatech.ac.kr (S.-Y.K.); Tel.: +82-041-560-1484 (S.-Y.K.)

[†] Dedicated to Prof. Dr. Karkala Vasantakumar Pai, Kuvempu University, on the occasion of his retirement.

[‡] Both the authors contributed equally to the work.



Citation: Shimoga, G.; Palem, R.R.; Choi, D.-S.; Shin, E.-J.; Ganesh, P.-S.; Saratale, G.D.; Saratale, R.G.; Lee, S.-H.; Kim, S.-Y. Polypyrrole-Based Metal Nanocomposite Electrode Materials for High-Performance Supercapacitors. *Metals* **2021**, *11*, 905. <https://doi.org/10.3390/met11060905>

Academic Editors: Leszek Adam Dobrzanski and Asit Kumar Gain

Received: 15 April 2021

Accepted: 29 May 2021

Published: 1 June 2021

Publisher's Note: MDPI stays neutral with regard to jurisdictional claims in published maps and institutional affiliations.



Copyright: © 2021 by the authors. Licensee MDPI, Basel, Switzerland. This article is an open access article distributed under the terms and conditions of the Creative Commons Attribution (CC BY) license (<https://creativecommons.org/licenses/by/4.0/>).

Abstract: Metallic nanostructures (MNs) and metal-organic frameworks (MOFs) play a pivotal role by articulating their significance in high-performance supercapacitors along with conducting polymers (CPs). The interaction and synergistic pseudocapacitive effect of MNs with CPs have contributed to enhance the specific capacitance and cyclic stability. Among various conjugated heterocyclic CPs, polypyrrole (PPy) (prevalently known as “synthetic metal”) is exclusively studied because of its excellent physicochemical properties, ease of preparation, flexibility in surface modifications, and unique molecular structure–property relationships. Numerous researchers attempted to improve the low electronic conductivity of MNs and MOFs, by incorporating conducting PPy and/or used decoration strategy. This was succeeded by fine-tuning this objective, which managed to get outstanding supercapacitive performances. This brief technical note epitomizes various PPy-based metallic hybrid materials with different nano-architectures, emphasizing its technical implications in fabricating high-performance electrode material for supercapacitor applications.

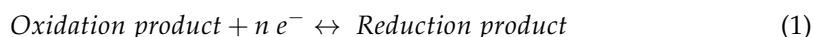
Keywords: conducting polymers; cyclic voltammetry; electrode materials; metal oxides; polypyrrole; supercapacitors; synthetic metal

1. Background

Modern advancements in the field of flexible electronics have been actively involved in design strategies to replace conventional inorganic semiconductors by organic and hybrid inorganic materials [1]. In this context, conjugated organic polymers, along with complementary metallic nanostructures (MNs), have been receiving much attention as promising hybrid components for flexible electronics [2]. It was an exciting moment for the scientific community in December 2000, as the pioneering joint research works of three scientists, namely Alan J. Heeger, Alan G. MacDiarmid, and Hideki Shirakawa, collectively received the Nobel Prize in Chemistry for the discovery and the development of conductive polymers (CPs), [3]. Due to ease of fabrication, mechanical robustness, chemical resistance, excellent electrochemical properties, and comparatively high conductivity ($>10^3 \text{ S cm}^{-1}$), these CPs have crucial importance in emerging energy storage device applications as an

active material. In particular, to construct advanced energy storage systems (ESSs), such as batteries and supercapacitors, functional CPs are directly incorporated as one of the energy storage active materials in addition to inorganic hybrid nanocomposites [4,5].

Depending on the charge transfer mechanism, supercapacitors can be technically categorized into two major types, namely (i) electric double layer supercapacitors (EDLCs) and (ii) pseudocapacitors. In the former case, there is no redox process (non-Faradaic charge transfer) involved, i.e., the charges are stored progressively in the electric double layer formed at the electrode's and electrolyte's interface, whereas in the latter type, a series of reversible and fast sequence of redox reactions (see Equation (1), note: n = integer and e^- = electron) (Faradaic charge transfer) can be noticed on the electroactive surfaces:



Comparatively, pseudocapacitors can accumulate greater electrochemical storage electricity and demonstrate higher energy density than EDLCs (for an illustration, see Figure 1). Accordingly, the synergistic and tunable complimenting properties of diverse nanoarchitecture metal-organic frameworks (metal oxides/phosphides/sulfides) with conjugated organic polymers, especially polypyrrole (PPy) derivatives, have found widespread application in fabricating electrochemical sensors and energy storage technologies [6–9].

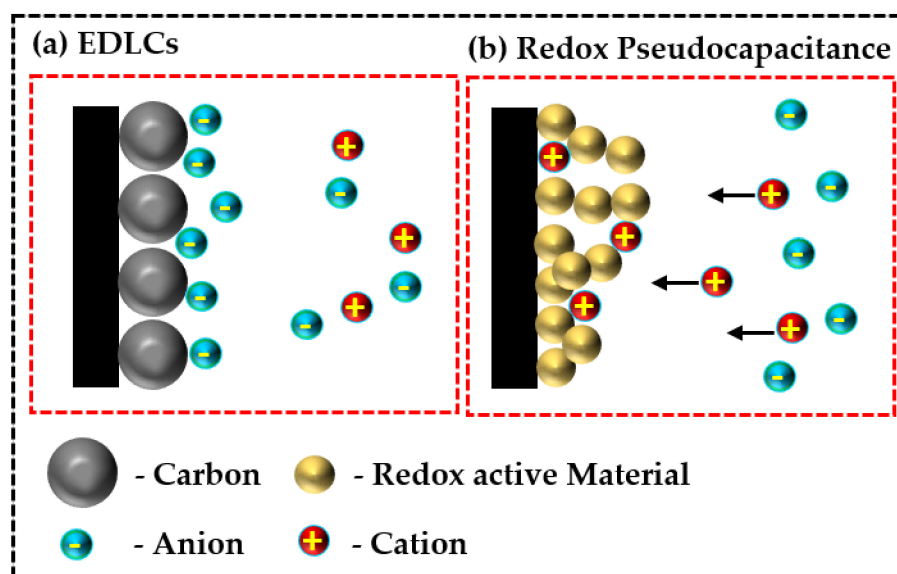


Figure 1. Schematic illustration of (a) electric double layer supercapacitors (EDLCs) and (b) redox pseudocapacitors.

The pioneering research works on PPy from chemical, electrochemical routes by Bocchi and coworkers [10] and Gardini [11] was a remarkable invention, and it contributed exceptional impact to PPy chemistry. Subsequently, plentiful research works are documented on PPy derivatives. In 2006, Akar and coworkers [12] documented optimized polymerization parameters to achieve PPy and its block copolymers with conductivities up to 4000 S cm^{-1} . The authors claim that the properties of these block copolymers of α,ω -diamine polydimethylsiloxane (DA-PDMS) and PPy can be regulated by adopting ratio parameters to attain unique morphology with ceric ammonium nitrate as an oxidizing agent [12]. Pyrrole is a sensitive organic compound known for its rapid aerial oxidation to form autoxidized red tar compounds. The rapidity of aerial oxidation is even quicker when the electronic donating groups are its substituents [13]. Despite its sensitiveness and reactivity, pyrroles can skillfully be oxidized to achieve PPy. The unique electronic properties and conductivities of PPy were enough to share the title as “organic metal/synthetic metal/metallic polymer” among other prominent conducting polymers [14].

The literature survey reveals that PPy exists as conducting salt. Deprotonation reaction is feasible after treatment with base, resulting in less conducting or insulating PPy base. The researchers proposed that the molecular structure of deprotonated PPy could encompass both reduced and oxidized forms of pyrrole subunit. Although the presence of polarons and unpaired spins are identified using electron spin resonance (ESR) spectroscopy along with localized positive charges on PPy, the hypothesis about conduction mechanisms is still in contention. The molecular structures of conducting/insulating PPy and rearrangement of electrons in PPy salt for the probable creation of polarons are sketched in Figure 2 [15–18]. Despite semiconducting properties, other CP families, such as polyaniline (PANi), polythiophene (PT) and poly(3,4-ethylene dioxythiophene) (PEDOT), are also well-exhibited pseudocapacitance behaviors. The controlled physicochemical/electrical properties and ease of synthesis make them an ideal material for energy storage applications. To the best of our knowledge, we are the first reporting a concise report that specifically reveals PPy-based metal nanocomposite electrode materials for high-performance supercapacitors.

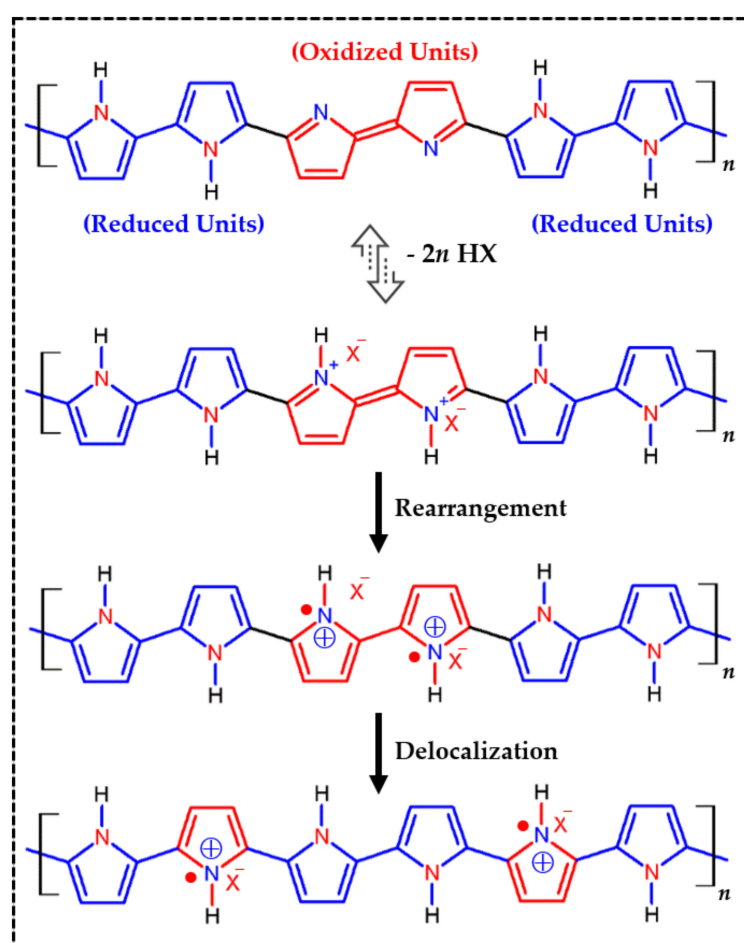


Figure 2. Deprotonation reaction of conducting PPy salt under alkaline conditions and rearrangement of electrons in PPy, generation of bipolarons/polarons by delocalization over PPy chain. Note: HX = arbitrary acid, X^- = corresponding counter ion, polarons = acts as charge carriers.

Concerning device construction strategies, both batteries and electrochemical capacitors follow similar prototypes but differ in energy storage mechanisms and applications. In brief, an electrical insulator (separator) often separates two electrodes (current collectors). The design strategy for electrolytic capacitors is usually represented as parallel plate capacitors; dielectric materials often separate the electrodes. The energy storage capability is because of polarization in the existence of an external electric field. Since the energy storage mechanism of electrochemical capacitors is in the capacitor of the electric double layer (an

interface between an electrode and an aqueous/non-aqueous electrolyte), the capacitance and energy density of these devices are compatibly larger than electrolytic capacitors. Although electrolytic capacitors have larger cycling efficacy, they suffer from low energy density. Hence, nanostructured CP electrodes with high surface area exhibiting a pronounced pseudocapacitance behavior are widely used to construct electrochemical capacitors [19–21]. Along with metal-organic frameworks (metal oxides/phosphides/sulfides), these nanostructured CPs display synergistic interaction, resulting in contributing superior supercapacitive properties. Figure 3 represents the device prototype of an electrochemical capacitor made of a CP electrode and its equivalent circuit illustration. Bryan et al. [22] recently briefly outlined the construction of electrochemical capacitors from various CPs and their device engineering strategies. The authors predominantly emphasized the pseudocapacitive performance of PPy with synthetic chemical doping strategies [22].

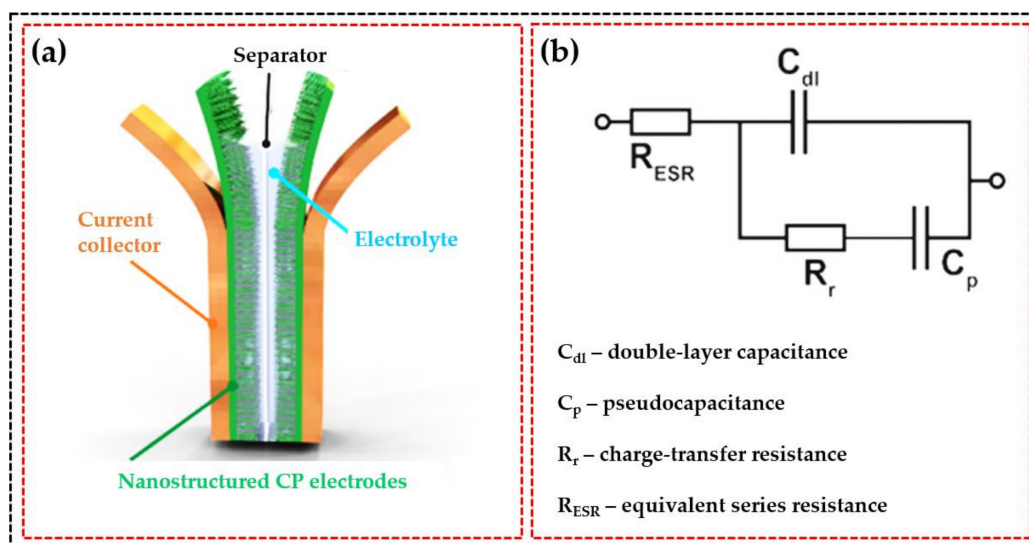


Figure 3. (a) Schematic illustration of a pseudocapacitor cell and (b) its equivalent circuit diagram that models the electrical behavior of the cell. Adopted with permission from [22], ACS, 2016.

Compared to EDLCs, ion transport in pseudocapacitors is indolent because of faradaic processes. Since CPs possess high electrochemical capacitance and conductivity, it must facilitate facile kinetics, charge carriers, charge mobility, and accessible counterions. By chemical reduction process (*n*-doping), the insertion of electrons to the conduction band will be carried out. Removal of electrons from the valence band was done by oxidation process (*p*-doping), which eventually upsurge the concentration of charge carriers [23,24]. Consider the ionization of CPs, there will be a difference in the equilibrium geometry of the ionized state and its respective ground state. The ionized state of CPs possesses lower equilibrium geometry than its ground state. This lattice distortion causes the highest occupied molecular orbital (HOMO) to swing upwards, and the lowest unoccupied molecular orbital (LUMO) shifts downwards, forming new energy bands in the bandgap. These newly created energy bands are delocalized over the polymer chain, results in the creation of a charge “island.” When the polymer chain is chemically doped, it results in ionization of polymer chains, and the overlapping and delocalization of these islands facilitates the conducting behavior of the polymers [25,26]. Since the conjugated sp^2 carbons are the key frameworks of CPs, the semi-metallic properties of CPs resemble the conductivities of 2D graphene or 3D graphite materials. Conversely, a Jahn–Teller-like relaxation (or Peierls transition) will ensure the separation among unfilled and filled portions of the sp^2 band. When graphene is chemically doped, it will also exhibit a bandgap. In contrast to graphene electronic conductivity, to demonstrate increased electronic conductivity in the case of CPs, new energy levels are essential, and they must be added to the gap via doping (see Figure 4 for a schematic illustration). The charge island formation in the case of CPs (especially PPy)

is a more divergent doping technique than that of conventional semiconductors [18,27,28]. Over the past few decades, the research works on metal-organic frameworks (MOFs) have gained increased importance in conventional gas separation and storage, catalysis, electrochemical sensors, and rechargeable batteries due to their unique surface characteristics, tunable porosities, and electrochemical properties. However, the application of MOFs in supercapacitor's electronic components is diminutive because of its high electrical resistivity. To fix this issue, decorating MOFs with a well-known conductive polymer, PPy (prevalently known as “synthetic metal”), can contribute favorable solicitations in the construction of electrochemical energy storage devices [29–33].

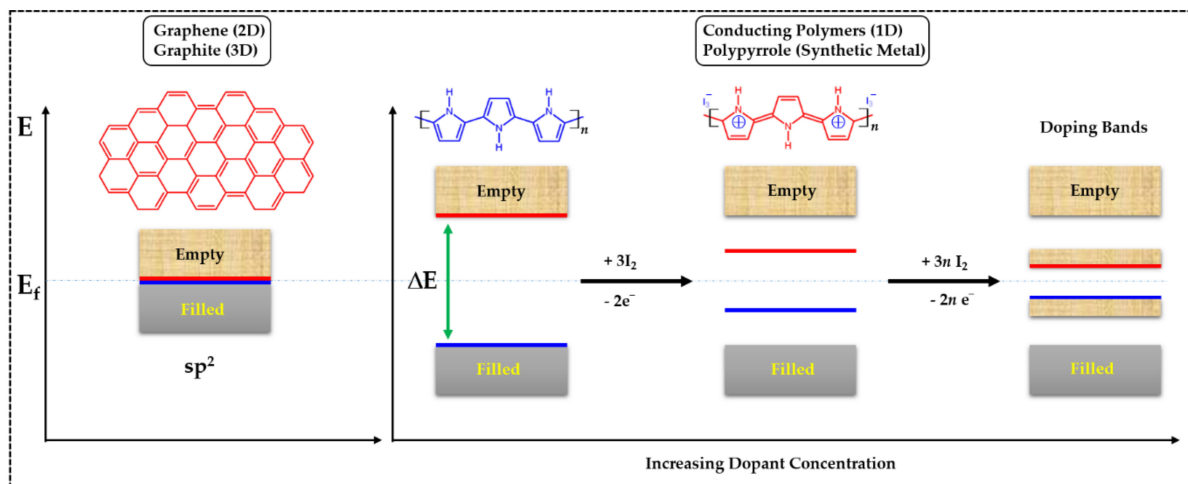


Figure 4. Unlike 2D graphene or 3D graphite, polypyrrole (PPy) has a distinct band gap leading to its semiconducting properties. In the chemical doping procedure of PPy, two electrons are removed from the polymer chain, creating a carbodication, or bipolaron, balanced by dopant counterions [23]. As the polymer is doped to its saturation limit, progressive bipolaronic states are formed. Their energy bands overlap, creating intermediate band structures that facilitate electronic transport throughout the PPy chain [24]. Adopted with permission from [22], ACS, 2016.

Depending on the peaks obtained from cyclic voltammograms, the specific capacitance (C_s) at different scan rates can be calculated by Equation (2):

$$C_s = \frac{\int IdV}{v \times m \times \Delta V} \quad (2)$$

where I is the response current in A, v is the scan rate in $V s^{-1}$, ΔV is the potential window in V and m is the mass of two active electrode material in g. In addition, from cyclic voltammograms of the charge/discharge curves, the specific capacitance (C_s) can be calculated from Equation (3):

$$C_s = 4 \frac{I \times \Delta t}{\Delta V \times M} \quad (3)$$

where I is the charge/discharge current in A, Δt is the discharge time in s, ΔV is the potential window in V and M is the total mass of active electrode material in g [34–37].

2. Polypyrrole-Based Hybrid Metallic Nanostructures as Electrode Materials for High Performance Supercapacitors

Hybrid metallic nanostructures embedded with PPy can exert noteworthy effects on the physico-chemical properties and the electrochemical properties due to the unique characteristics of both PPy and metallic nanostructures [38,39]. Since the booming progress in fabricating supercapacitor electrode materials from carbonaceous network structures has been proposed and studied by various researchers to accomplish the performances beyond the limitation of carbonaceous materials [40–42], Feng et al. [43] proposed nitrogen-doped porous carbon matrix complexed with PPy. The uniformly grown PPy nanospheres on

porous carbon matrix surface showed remarkably specific capacitance reaching a value of 237.5 F g^{-1} with 88.53% discharge after 1000 cycles. The complimenting characteristics of notable mechanical flexibility and high capacitance of PPy was utilized to develop wearable supercapacitors by growing nanotubular arrays with carbon nano-onions on fabric material [44]. These PPy-based hybrid nanostructures grown on fabric materials exhibited stretchable characteristics with superior energy storage capacitance (specific capacitance of 64.0 F g^{-1}). In addition, 99.0% capacitance was retained even at a strain of 50.0% after 500 stretching cycles [44].

Our main aim is to focus and provide a comprehensive inventory on PPy-based hybrid metallic nanostructures as supercapacitor electrodes; a systematic survey was carried out, and comparative metal-based PPy nanocomposite electrode parameters concerning supercapacitor applications are documented. By using electrospinning technique, Li et al. [45] successfully fabricated the hollow V_2O_5 fibers by the emulsion of vanadyl acetylacetonate, polyvinylpyrrolidone and polystyrene in N, N-dimethyl formamide followed by sintering in air at 430°C for 30 min. Furthermore, in order to achieve hollow, capsular PPy fibers on V_2O_5 , two-step vapor-phase polymerization technique was adopted and the electrodes showed appreciable specific capacitance of 203.0 mV s^{-1} with over 90.0% capacitance retention after 11,000 cycles at 10.0 A g^{-1} [45]. Dubal et al. [46] reported an inexpensive and straightforward electrodeposition protocol to synthesize nano-brick structures of PPy on stainless steel (SS) substrate. The deposition of PPy nano-bricks was achieved potentiostatically at $+0.9 \text{ V/SCE}$ for 2 min. These 3D nano-brick PPy structures showed appreciable electrochemical reversibility and a large specific capacitance of 476.0 F g^{-1} [46]. Shinde et al. [47] put forward a new cost-effective chemical bath deposition (CBD) method to synthesize PPy thin film on SS substrate. These instantly grown additive-free and binderless PPy thin films showed maximum achieved specific capacitance value 329.0 F g^{-1} at 5.0 mV s^{-1} . Furthermore, the low equivalent series resistance ($R_s = 1.08 \Omega$) value reflects negligible ohmic potential drop during the discharge process [47]. Since smartly tailored SS mesh shows superior stretchability, Huang et al. [48] fabricated PPy-based solid-state supercapacitors by electrochemically polymerizing pyrrole monomer. The fabricated supercapacitors showed an initial capacitance of 170.0 F g^{-1} at a relaxed state and 214.0 F g^{-1} at a 20% strain (at a specific current of 0.5 A g^{-1}) [48].

The fabrication of silver nanoparticles/nanoclusters-decorated hybrid PPy (Ag@PPy) nanocomposites were done by Gan et al. [49]. The hybrid Ag@PPy nanocomposites demonstrated an enhanced specific capacitance of 414 F g^{-1} compared to that of the pure PPy electrode (273 F g^{-1}). Fine-sized (2–4 nm) silver nanoparticles were initially distributed homogeneously on PPy, which effectually improved the electron hopping system PPy, thus enhancing the capacitance of the PPy. Medium-sized silver nanoparticles (55–100 nm) adhered to the PPy surface, acting as a spacer that minimizes the restacking of PPy. Furthermore, the transport pathway for electrons was shortened by this unique morphology, leading to improved cycling stability and specific capacitance of hybrid Ag@PPy nanocomposites [49]. Iqbal et al. [50] performed the oxidative chemical polymerization of pyrrole monomer in FeCl_3 as an oxidant. The authors also prepared the binary (Co_3O_4 @PPy) and ternary (Ag/ Co_3O_4 @PPy) nanocomposites, in situ synthesis of Co_3O_4 nanograins and silver nanoparticles along with PPy. The authors revealed spherical, tubular and globular appearances of PPy with Co_3O_4 and silver nanoparticles (some nanoparticles were also embedded inside the PPy structures). The authors showed that the ternary nanocomposites (Ag/ Co_3O_4 @PPy) demonstrated highest specific capacitance of 355.64 C g^{-1} compared to binary (Co_3O_4 @PPy) nanocomposite (280.68 C g^{-1}) and pure PPy (143.28 C g^{-1}) [50].

Although the high theoretical capacity of pseudocapacitive transition-metal oxides/hydroxides is promising for supercapacitor electrodes, they suffer severely from lower electrical conductivity and specific capacitance; this is why they are not often used in practical applications [51–53]. In concern to this, Mao et al. [50] designed one-dimensional silver nanowires (AgNWs) with hierarchical nanostructured $\text{Ni}(\text{OH})_2$ archi-

texture. These coaxial hierarchical core-shell structured AgNW@Ni(OH)₂@PPy hybrid electrode materials exhibited outstanding specific capacitance of 3103.5 F g^{−1} at 2.6 A g^{−1}. To date, this comprehensive performance has been reported to belong dedicatedly to the hybrid Ni(OH)₂ systems with PPy [54].

A thin-film electrode composed of ceramic oxide and yttrium aluminum garnet (YAG: Al₅Y₃O₁₂) with PPy was developed by Ehsani et al. [55]. This new type of film electrode was fabricated using pulse electrochemical deposition technology, and the electrodes showed enhanced specific capacitance (254.0 F g^{−1}) compared to a pure PPy electrode (109.0 F g^{−1}). The authors also discussed the stability advantages of these thin-film electrodes in aqueous electrolytes over commonly used ruthenium-based perovskites [55]. Previous investigations by Ariyanayagamkumarappa and Zhitomirsky showed that chromotropic acid (CHR) is an auspicious dopant material for the preparation of PPy. The PPy films synthesized using CHR dopant showed the highest specific capacitance of 343.0 F g^{−1} at 2.0 mV s^{−1} [56]. With these inspiring results, Zhu et al. [57] studied the influence of 2,7-Bis(2-sulfophenylazo)chromotropic acid tetrasodium salt (CHR-BS) on the supercapacitor behavior of fabricated PPy electrodes. The CHR-BS doped PPy electrodes showed elite capacitive retention of 109.9% even after 1000 cycles [57] (for the chemical structures of CHR and CHR-BS dopants, please see Figure 5).

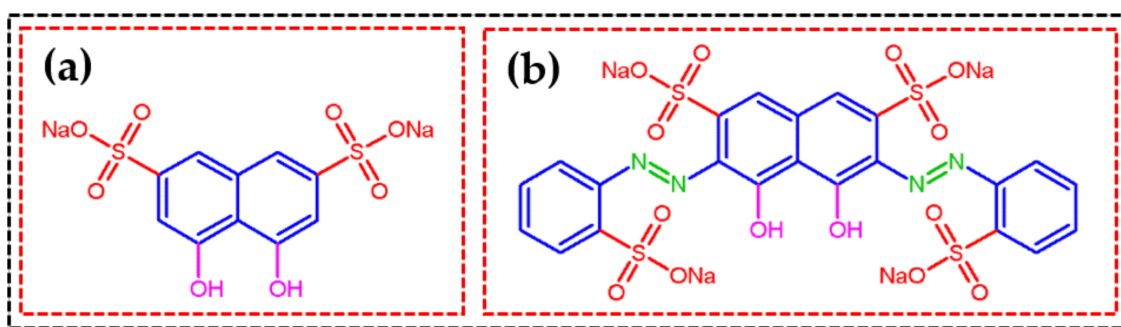


Figure 5. The chemical structures of (a) chromotropic acid (CHR) disodium salt and (b) 2,7-Bis(2-sulfophenylazo)chromotropic acid tetrasodium salt (CHR-BS).

By combining solvothermal reaction and electrodeposition technique, Yang et al. [58] developed hybrid nanosheet arrays having Co₃O₄ as a core and PPy as a shell. The electrode (Co₃O₄@PPy) made of Co₃O₄ and PPy showed unique synergistic effects and exhibited a large capacitance of 2.11 F cm^{−2} at a current density of 2.0 mA cm^{−2}. Furthermore, the equivalent series resistance value of the Co₃O₄@PPy hybrid electrode (0.238 Ω) is pointedly inferior to that of the new Co₃O₄ electrode (0.319 Ω) [58]. The ternary nanocomposites developed by Wei et al. [59] were done by electropolymerizing PPy onto flower-like cobalt oxide (f-Co₃O₄) morphological structures coating uniformly on carbon paper (CP). These ternary nanocomposites demonstrated more extended stability in 2.0 M aqueous KOH with a specific capacitance of 398.4 F g^{−1} [59]. To improve the electrochemical performances, Wang et al. [60] proposed the ternary core-shell hetero-structured composites composed of Co₃O₄@PPy@MnO₂, which show a remarkable specific capacitance of 782.0 F g^{−1} at 0.5 A g^{−1}. The hybrid composites made of MWCNTs with PPy and Co₃O₄ show high electrochemical performances, with only 2.9% loss of their initial capacitance after 5000 cycles [61]. Since metal sulfides are promising electrode materials for supercapacitor applications, Cheng et al. [62] considered individual synergistic effects of Co₃S₄ and PPy to construct a hybrid with tangled conductive networks of Co₃S₄ hollow nanocages (HNCs) with PPy and studied its merits as supercapacitor electrodes. The Co₃S₄-HNCs@PPy hybrid nanocomposites showed extendable durability with an outstanding specific capacitance of 1706.0 F g^{−1} at 1.0 A g^{−1} [62].

Diverse research reports have demonstrated the representative metal nanoarchitectures hybrid composites with PPy network including oxides, phosphides, sulfides etc.

The appreciable specific capacitance demonstrated by these PPy-Metal hybrid nanocomposites signifies that these electrode materials are the primary choice for supercapacitor applications. The research contribution involving a variety of hybrid nanocomposites along with PPy were succinctly tabulated in Table 1 with its electrode parameters [41,45–50,55,57–122].

Table 1. Partial list of polypyrrole (PPy)-based fabricated metal nanocomposite electrodes and its parameters for high-performance supercapacitor applications.

Fabricated Electrode	Electrolyte	Specific Capacitance	Current Density/Scan Rate	Capacitance Retention/Cycling Stability	References
PPy on hollow V ₂ O ₅ fibers	1.0 M H ₂ SO ₄	203.0 F g ^{−1}	2.0 mV s ^{−1}	>90.0% after 11,000 cycles at 10.0 A g ^{−1}	[45]
PPy nanobricks on SS substrate	0.5 M H ₂ SO ₄	476.0 F g ^{−1}	5.0 mA cm ^{−2}	89.0% charge/discharge efficiency	[46]
PPy thin film on SS substrate	0.5 M H ₂ SO ₄	329.0 F g ^{−1}	5.0 mV s ^{−1}	-	[47]
PPy on a knitted SS mesh	^a H ₃ PO ₄ -PVA	^b 214.0 F g ^{−1}	0.5 A g ^{−1}	98.0% after 10,000 cycles	[48]
Ag@PPy	1.0 M H ₂ SO ₄	^c 414.0 F g ^{−1}	0.2 A g ^{−1}	98.9% after 1000 cycles at 0.5 A g ^{−1}	[49]
PPy	1.0 M KOH	143.28 C g ^{−1}	1.4 A g ^{−1}	-	[50]
Co ₃ O ₄ @PPy	1.0 M KOH	280.68 C g ^{−1}	1.4 A g ^{−1}	-	[50]
Ag/Co ₃ O ₄ @PPy	1.0 M KOH	355.64 C g ^{−1}	1.4 A g ^{−1}	153.67% after 3000 cycles	[50]
AgNW@Ni(OH) ₂ @PPy	6.0 M KOH	3103.5 F g ^{−1}	2.6 A g ^{−1}	92.18% after 20,000 cycles	[50]
PPy	0.1 M H ₂ SO ₄	109.0 F g ^{−1}	25.0 mV s ^{−1}	30.0% after 20,000 cycles	[55]
PPy-Al ₅ Y ₃ O ₁₂	0.1 M H ₂ SO ₄	254.0 F g ^{−1}	25.0 mV s ^{−1}	85.0% after 20,000 cycles	[55]
CHR-BS doped PPy	0.5 M Na ₂ SO ₄	7.2 F cm ^{−2}	2.0 mV s ^{−1}	109.9% after 1000 cycles at 0.7 A g ^{−1}	[57]
Co ₃ O ₄ @PPy core-shell	1.0 M KOH	2.11 F cm ^{−2}	2.0 mA cm ^{−2}	85.0% after 5000 cycles	[58]
^d PPy/f-Co ₃ O ₄ /CP	2.0 M KOH	398.4 F g ^{−1}	0.2 A g ^{−1}	Negligible loss after 1000 cycles	[59]
Co ₃ O ₄ @PPy@MnO ₂	1.0 M KOH	782.0 F g ^{−1}	0.5 A g ^{−1}	97.6% after 2000 cycles at 5.0 A g ^{−1}	[60]
Co ₃ O ₄ /MWCNT/@PPy	6.0 M KOH	609.0 F g ^{−1}	3.0 A g ^{−1}	97.1% after 5000 cycles	[61]
Co ₃ S ₄ -HNCs@PPy	2.0 M KOH	1706.0 F g ^{−1}	1.0 A g ^{−1}	82.8% after 10,000 cycles	[62]
PPy-CPSC	1.0 M H ₂ SO ₄	168.0 F g ^{−1}	2.0 mA cm ^{−2}	Stable after 2000 cycles	[63]
PPy-CuCo	0.1 M LiClO ₄	556.0 F g ^{−1}	1.0 A g ^{−1}	90.0% after 2000 cycles at 20.0 A g ^{−1}	[64]
PPy/CuO	0.5 M H ₂ SO ₄	20.78 F g ^{−1}	5.0 mV s ^{−1}	48.39% after 500 cycles at 100 mV s ^{−1}	[65]
PPy	1.0 M H ₂ SO ₄	174.0 F g ^{−1}	1.0 A g ^{−1}	62.83% after 3000 cycles	[66]
PPy/CuO/Eu ₂ O ₃	1.0 M H ₂ SO ₄	320.0 F g ^{−1}	1.0 A g ^{−1}	92.89% after 3000 cycles	[66]
CuS@PPy	1.0 M KCl	427.0 F g ^{−1}	1.0 A g ^{−1}	88.0% after 1000 cycles	[67]
PPy/CuS/BC	2.0 M NaCl	580.0 F g ^{−1}	0.8 mA cm ^{−2}	73.0% after 300 cycles	[68]
f-CNFs/PPy/MnO ₂	1.0 M KCl	409.88 F g ^{−1}	25.0 mV s ^{−1}	86.30% after 3000 cycles	[69]
PPy@Fe	0.3 M C ₂ H ₂ O ₄	2280.0 F g ^{−1}	3.0 mA cm ^{−2}	-	[70]
T-Fe ₂ O ₃ /PPy NAs	^e PVA-LiCl	382.4 mF cm ^{−2}	0.5 mA cm ^{−2}	97.2% after 5000 cycles	[71]
PPy@Fe ₂ O ₃	3.0 M KCl	560.0 F g ^{−1}	5.0 A g ^{−1}	97.3% after 20,000 cycles at 40.0 A g ^{−1}	[72]
PPy/GNS/Eu ³⁺	1.0 M H ₂ SO ₄	238.0 F g ^{−1}	1.0 A g ^{−1}	-	[73]
PPy/GO-HT	1.0 M H ₂ SO ₄	198.0 F g ^{−1}	20.0 A g ^{−1}	92.0% after 3000 cycles	[41]
WO ₃ /PPy/G	0.5 M H ₂ SO ₄	513.0 F g ^{−1}	5.0 mV s ^{−1}	87.3% after 1000 cycles at 10.0 A g ^{−1}	[74]
PPy-H ₄ [PVMo ₁₁ O ₄₀]	0.1 M H ₂ SO ₄	561.1 F g ^{−1}	0.2 A g ^{−1}	95.0% after 4500 cycles	[75]
MgCo ₂ O ₄ @PPy/NF	2.0 M KOH	1079.6 F g ^{−1}	1.0 A g ^{−1}	97.4% after 1000 cycles	[76]
PPy@MnCo ₂ O ₄	6.0 M KOH	2364.0 F g ^{−1}	5.0 mV s ^{−1}	85.5% after 10,000 cycles	[77]
PPy@MnMoO ₄	6.0 M KCl	374.8 F g ^{−1}	0.2 A g ^{−1}	80.6% after 10,000 cycles	[78]
PPy@MnMoO ₄ /CFs	0.6 M H ₂ SO ₄	302.0 F g ^{−1}	1.0 A g ^{−1}	83.0% after 10,000 cycles at 2.0 A g ^{−1}	[79]
MnO ₂ @PPy coaxial nanotubes	1.0 M Na ₂ SO ₄	380.0 F g ^{−1}	50.0 mV s ^{−1}	90.0% after 1000 cycles	[80]
MnO ₂ /PPy nanotubular	2.0 M KCl	337.0 F g ^{−1}	0.5 A g ^{−1}	90.6% after 1000 cycles	[81]
PPy/MnO ₂	1.0 M Na ₂ SO ₄	141.6 F g ^{−1}	2.0 mA cm ^{−2}	73.0% after 500 cycles	[82]
MnO ₂ /PPy	1.0 M KCl	273.0 F g ^{−1}	0.5 A g ^{−1}	-	[83]
MnO ₂ /PPy	1.0 M Na ₂ SO ₄	205.0 F g ^{−1}	2.0 mV s ^{−1}	96.5% after 400 cycles	[84]

Table 1. Cont.

Fabricated Electrode	Electrolyte	Specific Capacitance	Current Density/Scan Rate	Capacitance Retention/Cycling Stability	References
PPy/MnO ₂	1.0 M Na ₂ SO ₄	325.0 F g ⁻¹	0.2 A g ⁻¹	96.0% after 1000 cycles 1.0 A g ⁻¹	[85]
MnO ₂ /PPy	0.5 M Na ₂ SO ₄	625.0 F g ⁻¹	0.5 A g ⁻¹	96.4% after 1000 cycles	[86]
PPy/MnO ₂ /CNTs	1.0 M Na ₂ SO ₄	402.7 F g ⁻¹	1.0 A g ⁻¹	96.2% after 1000 cycles	[87]
PYMG-HT (PPy/MnO ₂ /GT)	0.5 M Na ₂ SO ₄	821.3 F g ⁻¹	0.5 A g ⁻¹	-	[88]
MnO ₂ /PPy/TSA	0.5 M Na ₂ SO ₄	376.0 F g ⁻¹	3.0 mA cm ⁻²	90.0% after 500 cycles at 5.0 mA cm ⁻²	[89]
MoO ₃ /PPy	1.0 M Na ₂ SO ₄	129.0 F g ⁻¹	1.0 A g ⁻¹	90.0% after 200 cycles at 0.67 A g ⁻¹	[90]
PPy/MoS ₂ /PTFE	1.0 M KCl	553.7 F g ⁻¹	1.0 A g ⁻¹	90.0% after 500 cycles	[91]
MoS ₂ /PPy	0.5 M Na ₂ SO ₄	462.0 F g ⁻¹	1.0 A g ⁻¹	82.0% after 2000 cycles 3.0 A g ⁻¹	[92]
PPy-MOx	0.1 M H ₂ SO ₄	463.0 F g ⁻¹	-	-	[93]
Ni(Cu)PPy	1.0 M KOH	659.52 F g ⁻¹	5.0 mV s ⁻¹	87.0% after 1000 cycles	[94]
Ni(OH) ₂ /PNTs	6.0 M KOH	864.0 F g ⁻¹	1.0 A g ⁻¹	91.1% after 2000 cycles at 5.0 A g ⁻¹	[95]
PPy-Ni(OH) ₂ nanowires	1.0 M LiSO ₄ and 0.19 M DHB	75.0 F cm ⁻²	20.0 mV s ⁻¹	87.0% after 100 cycles	[96]
Ni _{1/3} Co _{2/3} (CO ₃) _{0.5} OH _{0.11} H ₂ O/PPy	2.0 M KOH	964.8 F g ⁻¹	1.0 A g ⁻¹	80.2% after 5000 cycles at 5.0 A g ⁻¹	[97]
PPy/Ni ₂ P	1.0 M Na ₂ SO ₄	476.5 F g ⁻¹	1.0 A g ⁻¹	89.0% after 3000 cycles	[98]
PPy@NiCo(OH) ₂	^f PVA-KOH	1469.25 F g ⁻¹	1.0 A g ⁻¹	95.2% after 10,000 cycles 30.0 A g ⁻¹	[99]
CF@NiCo ₂ O ₄ @PPy core-shell	3.0 M KOH	1.44 F cm ⁻²	2.0 mA cm ⁻²	85.0% after 5000 cycles at 10.0 mA cm ⁻²	[100]
PNTs@NiCo ₂ S ₄	6.0 M KOH	911.0 F g ⁻¹	1.0 A g ⁻¹	93.2% after 4000 cycles at 5.0 A g ⁻¹	[101]
PPy@NiCo ₂ S ₄	2.0 M KOH	908.1 F g ⁻¹	1.0 A g ⁻¹	87.7% after 2000 cycles	[102]
NiCo ₂ S ₄ @PPy/NF	3.0 M KOH	9.781 F cm ⁻²	5.0 mA cm ⁻²	80.64% after 2500 cycles at 50.0 mA cm ⁻²	[103]
NiFe ₂ O ₄ /PPy	1.0 M H ₂ SO ₄	721.66 F g ⁻¹	10.0 mV s ⁻¹	97.24% after 1000 cycles	[104]
NiMn-LDH/PPy/BC	2.0 M KOH	1427.0 F g ⁻¹	1.0 A g ⁻¹	66.75% after 2000 cycles at 10.0 A g ⁻¹	[105]
CoAl-LDH/PPy/Graphene	30 wt % KOH	864.0 F g ⁻¹	1.0 A g ⁻¹	90.1% after 10,000 cycles	[106]
PPy@CoNi-LDH/RGO	1.0 M KOH	2342.0 F g ⁻¹	1.0 A g ⁻¹	115.4% after 20,000 cycles	[107]
NiAl-LDH@GO-PPy	1.0 M KOH	845.0 F g ⁻¹	2.0 mV s ⁻¹	92.0% after 5000 cycles	[108]
Ni-MOF@PPy	3.0 M KOH	715.6 F g ⁻¹	0.3 A g ⁻¹	80.0% after 10,000 cycles	[109]
NiO@NMWCNT/PPy	2.0 M KOH	395.0 F g ⁻¹	0.5 A g ⁻¹	90.0% after 5000 cycles	[110]
NiO/CS-PPy nanotube	1.0 M KOH	934.11 F g ⁻¹	1.0 A g ⁻¹	84.90% after 10,000 cycles	[111]
PPy/NiS/BC	2.0 M NaCl	713.0 F g ⁻¹	0.8 mA cm ⁻²	-	[112]
MoS ₂ -rGO/PPy NTs (ITO coated glass)	1.0 M KCl	1561.0 F g ⁻¹	1.0 A g ⁻¹	72.0% after 10,000 cycles at 10.0 A g ⁻¹	[113]
MoS ₂ -rGO/PPy NTs (irradiated, 100.0 MeV O ⁷⁺)	1.0 M KCl	1875.0 F g ⁻¹	1.0 A g ⁻¹	91.0% after 10,000 cycles at 10.0 A g ⁻¹	[114]
PPy/RGO/Fe ₂ O ₃	1.0 M KCl	125.7 F g ⁻¹	0.5 A g ⁻¹	81.3% after 200 cycles	[115]
RuOx-PPy	0.1 M H ₂ SO ₄	681.0 F g ⁻¹	1.0 mA cm ⁻²	87.2% after 1000 cycles	[116]
PPy/Sm ₂ O ₃	1.0 M NaNO ₃	771.0 F g ⁻¹	20.0 mA cm ⁻²	47.0% after 800 cycles	[117]
PPy/SWCNT/TiO ₂	1.0 M KCl	282.0 F g ⁻¹	10.0 mV s ⁻¹	63.9% after 1000 cycles	[118]
PPy/TiO ₂	1.0 M KCl	247.0 F g ⁻¹	1.0 mA cm ⁻²	-	[119]
V ₂ O ₅ -PPy	5.0 M LiCl	412.0 F g ⁻¹	4.5 mA cm ⁻²	80.0% after 5000 cycles	[120]
ZnCo ₂ O ₄ /PPy	3.0 M KOH	1559.0 F g ⁻¹	2.0 mA cm ⁻²	90.0% after 5000 cycles at 10.0 mA cm ⁻²	[121]
ZnO/PPy	1.0 M LiClO ₄	131.22 F g ⁻¹	-	88.0% after 5000 cycles	[122]

PPy = Polypyrrole, DHB = 1,4-dihydroxybenzene, SS = stainless steel, CHR-BS = 2,7-Bis(2-sulfophenylazo)chromotropic acid tetrasodium salt, CP = carbon paper, HNCs = hollow nanocages, MWCNT = multiwall carbon nanotube, f-CNFs = functionalized carbon nanofibers, CPSC = conductive polymer-based supercapacitor, CF = carbon fibers, NF = nickel foam, NAs = nano arrays, BC = bacterial cellulose, CS = chitosan, HT = hydrothermal, PNTs = polypyrrole nanotubes, SWCNT = single-wall carbon nanotube, MOF = metal-organic-framework, RGO = reduced graphene oxide, LDH = layered double hydroxides, TSA = p-toluenesulfonic acid, PTFE = polytetrafluoroethylene, ^a = gel electrolyte made of 6.0 g H₃PO₄ and 6.0 g PVA in 60.0 mL deionized water (also serving as a separator), ^b = at a 20% strain, ^c = specific capacitances increased from 273.0 to 414.0 F g⁻¹ when the AgNO₃ concentration was increased from 0 to 0.05 M, ^d = ternary composites composed of PPy, flower such as Co₃O₄, and CP, ^e = 4.24 g of LiCl and 2.0 g of PVA were added in 20 mL deionized water and heated at 85 °C to make a gel electrolyte, ^f = 3.0 g KOH was dissolved in 30 mL purified water then 3.0 g polyvinyl alcohol (PVA) was slowly added in to form a gel solution.

3. Concluding Remarks

To curtail the environmental and economic effects instigated by the exhaustion of non-renewable energy sources, the use of the most demanding green renewable energy storage devices is intensified, expressly supercapacitors. To summarize, there are several advantages encountered experimentally by using PPy with metal nano architectures as supercapacitor electrode materials that can be helpful in practical device applications. With suitable methods (hydrothermal, in situ polymerization along with metallic nanostructures) and successful implementation of synthetic strategies, this would provide access to develop various nano architectures with diverse physico-chemical properties. In recent years, supercapacitors have attracted a great deal of interest and have emerged as an embedded system for Internet of Things (IoT) applications [123]. Due to its unique high energy density and remarkable power efficiency characteristics, supercapacitors could hold a very high electrical charge, replacing the use of batteries in tiny portable devices.

Author Contributions: Conceptualization, methodology, validation, writing original draft, G.S.; methodology, validation, R.R.P.; manuscript review and editing, D.-S.C., E.-J.S., G.D.S., R.G.S. and P.-S.G.; manuscript review and final editing, S.-H.L.; manuscript review, final editing and supervision, S.-Y.K. All authors have read and agreed to the published version of the manuscript.

Funding: This work was supported by the Priority Research Centers Program through the National Research Foundation of Korea (NRF) funded by the Ministry of Education (NRF-2018R1A6A1A03025526). This work was supported by a National Research Foundation of Korea (NRF) grant funded by the Ministry of Education (NRF-2020R1I1A3065371). This work was also supported by the Technology Innovation Program (10077367, Development of a film-type transparent /stretchable 3D touch sensor /haptic actuator combined module and advanced UI/UX) funded by the Ministry of Trade, Industry & Energy (MOTIE, Korea).

Institutional Review Board Statement: Not applicable.

Informed Consent Statement: Not applicable.

Data Availability Statement: Not applicable.

Conflicts of Interest: The authors declare no conflict of interest.

References

- Ocheje, M.U.; Charron, B.P.; Nyayachavadi, A.; Rondeau-Gagné, S. Stretchable electronics: Recent progress in the preparation of stretchable and self-healing semiconducting conjugated polymers. *Flex. Print. Electron.* **2017**, *2*, 043002. [CrossRef]
- Wang, M.; Baek, P.; Akbarinejad, A.; Barker, D.; Travas-Sejdic, J. Conjugated polymers and composites for stretchable organic electronics. *J. Mater. Chem. C* **2019**, *7*, 5534–5552. [CrossRef]
- The Nobel Prize. The Nobel Prize in Chemistry 2000. Available online: <https://www.nobelprize.org/prizes/chemistry/2000/summary/> (accessed on 16 December 2020).
- Naresh, U.; Kumar, R.J.; Ramesh, S.; Chandra Babu Naidu, C.B.K.; Basha, D.B.; Banerjee, P.; Srinivas, K. Conducting Polymer Derived Materials for Batteries. In *Conducting Polymers-Based Energy Storage Materials*; Inamuddin, Boddula, R., Ahmer, M.F., Asiri, A.M., Eds.; CRC Press; Taylor & Francis Group: Abingdon, UK, 2019; Chapter 3; pp. 65–78.
- Kumar, A.B.V.K.; Chaudhary, S.; Ramana, C.H.V.V. Conducting Polymer-Metal-Based Binary Composites for Supercapacitor Applications. In *Conducting Polymers-Based Energy Storage Materials*; Inamuddin, Boddula, R., Ahmer, M.F., Asiri, A.M., Eds.; CRC Press; Taylor & Francis Group: Abingdon, UK, 2019; Chapter 14; pp. 209–234.
- Pal, B.; Yang, S.; Ramesh, S.; Thangadurai, V.; Jose, R. Electrolyte selection for supercapacitive devices: A critical review. *Nanoscale Adv.* **2019**, *1*, 3807–3835. [CrossRef]
- Kim, B.K.; Sy, S.; Yu, A.; Zhang, J. Electrochemical Supercapacitors for Energy Storage and Conversion. In *Handbook of Clean Energy Systems*; John Wiley and Sons: Hoboken, NJ, USA, 2015; pp. 1–25.
- Huang, S.; Zhu, X.; Sarkar, S.; Zhao, Y. Challenges and opportunities for supercapacitors. *APL Mater.* **2019**, *7*, 100901. [CrossRef]
- Patterson, N.; Xiao, B.; Ignaszak, A. Polypyrrole decorated metal–organic frameworks for supercapacitor devices. *RSC Adv.* **2020**, *10*, 20162–20172. [CrossRef]
- Dall’Olio, A.; Dascola, G.; Varraca, V.; Bocchi, V. Electron paramagnetic resonance and conductivity of an electrolytic oxy-purrole black. *Gazz. Chim. Ital.* **1961**, *46*, 279, OCLC Number: 28804047.
- Gardini, G. The Oxidation of Monocyclic Pyrroles. *Adv. Heterocycl. Chem.* **1973**, *15*, 67–98. [CrossRef]
- Kızılcan, N.; Öz, N.K.; Ustamehmetoglu, B.; Akar, A. High conductive copolymers of polypyrrole- α,ω -diamine polydimethylsiloxane. *Eur. Polym. J.* **2006**, *42*, 2361–2368. [CrossRef]

13. Jones, R.A.; Bean, G.P. Oxidation and Reduction of the Pyrrole Ring. In *Organic Chemistry: A Series of Monographs*; Elsevier BV: Amsterdam, The Netherlands, 1977; Volume 34, Chapter 5; pp. 209–247.
14. Kanazawa, K.K.; Diaz, A.F.; Geiss, R.H.; Gill, W.D.; Kwak, J.F.; Logan, J.A.; Rabolt, J.F.; Street, G.B. 'Organic metals': Polypyrrole, a stable synthetic 'metallic' polymer. *J. Chem. Soc. Chem. Commun.* **1979**, *19*, 854–855. [\[CrossRef\]](#)
15. Pei, Q.; Qian, R. Protonation and deprotonation of polypyrrole chain in aqueous solutions. *Synth. Met.* **1991**, *45*, 35–48. [\[CrossRef\]](#)
16. Forsyth, M.; Truong, V.-T. A study of acid/base treatments of polypyrrole films using ^{13}C n.m.r. spectroscopy. *Polymer* **1995**, *36*, 725–730. [\[CrossRef\]](#)
17. Maksymiuk, K. Chemical Reactivity of Polypyrrole and Its Relevance to Polypyrrole Based Electrochemical Sensors. *Electroanalysis* **2006**, *18*, 1537–1551. [\[CrossRef\]](#)
18. Stejskal, J.; Trchová, M.; Bober, P.; Morávková, Z.; Kopecký, D.; Vršata, M.; Prokeš, J.; Varga, M.; Watzlová, E. Polypyrrole salts and bases: Superior conductivity of nanotubes and their stability towards the loss of conductivity by deprotonation. *RSC Adv.* **2016**, *6*, 88382–88391. [\[CrossRef\]](#)
19. Skyllas-Kazacos, M. Electro-chemical energy storage technologies for wind energy systems. In *Stand-Alone and Hybrid Wind Energy Systems*; Woodhead Publishing Series in Energy Elsevier: Amsterdam, The Netherlands, 2010; pp. 323–365. [\[CrossRef\]](#)
20. Rafik, F.; Gualous, H.; Gallay, R.; Crausaz, A.; Berthon, A. Frequency, thermal and voltage supercapacitor characterization and modeling. *J. Power Sources* **2007**, *165*, 928–934. [\[CrossRef\]](#)
21. Simon, P.; Gogotsi, Y. Materials for electrochemical capacitors. *Nat. Mater.* **2008**, *7*, 845–854. [\[CrossRef\]](#) [\[PubMed\]](#)
22. Bryan, A.M.; Santino, L.; Lu, Y.; Acharya, S.; D'Arcy, J.M. Conducting Polymers for Pseudocapacitive Energy Storage. *Chem. Mater.* **2016**, *28*, 5989–5998. [\[CrossRef\]](#)
23. Bredas, J.L.; Street, G.B. Polarons, bipolarons, and solitons in conducting polymers. *Accounts Chem. Res.* **1985**, *18*, 309–315. [\[CrossRef\]](#)
24. Mitchell, G.; Davis, F.; Legge, C. The effect of dopant molecules on the molecular order of electrically-conducting films of polypyrrole. *Synth. Met.* **1988**, *26*, 247–257. [\[CrossRef\]](#)
25. Kaner, R.B.; MacDiarmid, A.G. Plastics that Conduct Electricity. *Sci. Am.* **1988**, *258*, 106–111. [\[CrossRef\]](#)
26. Tourillon, G.; Garnier, F. Effect of dopant on the physicochemical and electrical properties of organic conducting polymers. *J. Phys. Chem.* **1983**, *87*, 2289–2292. [\[CrossRef\]](#)
27. Nevius, M.S.; Conrad, M.; Wang, F.; Celis, A.; Nair, M.N.; Taleb-Ibrahimi, A.; Tejeda, A.; Conrad, E.H. Semiconducting Graphene from Highly Ordered Substrate Interactions. *Phys. Rev. Lett.* **2015**, *115*, 136802. [\[CrossRef\]](#)
28. Kang, H.; Geckeler, K. Enhanced electrical conductivity of polypyrrole prepared by chemical oxidative polymerization: Effect of the preparation technique and polymer additive. *Polymer* **2000**, *41*, 6931–6934. [\[CrossRef\]](#)
29. Mehtab, T.; Yasin, G.; Arif, M.; Shakeel, M.; Korai, R.M.; Nadeem, M.; Muhammad, N.; Lu, X. Metal-organic frameworks for energy storage devices: Batteries and supercapacitors. *J. Energy Storage* **2019**, *21*, 632–646. [\[CrossRef\]](#)
30. Xu, G.; Nie, P.; Dou, H.; Ding, B.; Li, L.; Zhang, X. Exploring metal organic frameworks for energy storage in batteries and supercapacitors. *Mater. Today* **2017**, *20*, 191–209. [\[CrossRef\]](#)
31. Qi, K.; Hou, R.; Zaman, S.; Qiu, Y.; Xia, B.Y.; Duan, H. Construction of Metal–Organic Framework/Conductive Polymer Hybrid for All-Solid-State Fabric Supercapacitor. *ACS Appl. Mater. Interfaces* **2018**, *10*, 18021–18028. [\[CrossRef\]](#)
32. Simon, P.; Gogotsi, Y.; Dunn, B. Where Do Batteries End and Supercapacitors Begin? *Science* **2014**, *343*, 1210–1211. [\[CrossRef\]](#)
33. Das, T.K.; Prusty, S. Review on Conducting Polymers and Their Applications. *Polym. Technol. Eng.* **2012**, *51*, 1487–1500. [\[CrossRef\]](#)
34. Conway, B.E. *Electrochemical Supercapacitors: Scientific Fundamentals and Technological Applications*; Kluwer Academic/Plenum Publishers: New York, NY, USA, 1997.
35. Huang, L.; Chen, D.; Ding, Y.; Feng, S.; Wang, Z.L.; Liu, M. Nickel–Cobalt Hydroxide Nanosheets Coated on NiCo_2O_4 Nanowires Grown on Carbon Fiber Paper for High-Performance Pseudocapacitors. *Nano Lett.* **2013**, *13*, 3135–3139. [\[CrossRef\]](#) [\[PubMed\]](#)
36. Stoller, M.D.; Ruoff, R.S. Best practice methods for determining an electrode material's performance for ultracapacitors. *Energy Environ. Sci.* **2010**, *3*, 1294–1301. [\[CrossRef\]](#)
37. Hulicova-Jurcakova, D.; Puziy, A.M.; Poddubnaya, O.I.; Suárez-García, F.; Tascon, J.M.D.; Lu, G.Q. Highly Stable Performance of Supercapacitors from Phosphorus-Enriched Carbons. *J. Am. Chem. Soc.* **2009**, *131*, 5026–5027. [\[CrossRef\]](#)
38. Lv, H.; Pan, Q.; Song, Y.; Liu, X.-X.; Liu, T. A Review on Nano-/Microstructured Materials Constructed by Electrochemical Technologies for Supercapacitors. *Nano-Micro Lett.* **2020**, *12*, 1–56. [\[CrossRef\]](#)
39. Abdah, M.A.A.M.; Azman, N.H.N.; Kulandaivalu, S.; Sulaiman, Y. Review of the use of transition-metal-oxide and conducting polymer-based fibres for high-performance supercapacitors. *Mater. Des.* **2020**, *186*, 108199. [\[CrossRef\]](#)
40. Wang, J.; Li, X.; Du, X.; Wang, J.; Ma, H.; Jing, X. Polypyrrole composites with carbon materials for supercapacitors. *Chem. Pap.* **2017**, *71*, 293–316. [\[CrossRef\]](#)
41. Moyseowicz, A.; Pająk, K.; Gajewska, K.; Gryglewicz, G. Synthesis of Polypyrrole/Reduced Graphene Oxide Hybrids via Hydrothermal Treatment for Energy Storage Applications. *Materials* **2020**, *13*, 2273. [\[CrossRef\]](#) [\[PubMed\]](#)
42. Borenstein, A.; Hanna, O.; Attias, R.; Luski, S.; Brousse, T.; Aurbach, D. Carbon-based composite materials for supercapacitor electrodes: A review. *J. Mater. Chem. A* **2017**, *5*, 12653–12672. [\[CrossRef\]](#)
43. Feng, M.; Lu, W.; Zhou, Y.; Zhen, R.; He, H.; Wang, Y.; Li, C. Synthesis of polypyrrole/nitrogen-doped porous carbon matrix composite as the electrode material for supercapacitors. *Sci. Rep.* **2020**, *10*, 1–12. [\[CrossRef\]](#) [\[PubMed\]](#)

44. Wang, L.; Zhang, C.; Jiao, X.; Yuan, Z. Polypyrrole-based hybrid nanostructures grown on textile for wearable supercapacitors. *Nano Res.* **2019**, *12*, 1129–1137. [\[CrossRef\]](#)
45. Li, Z.; Cai, J.; Cizek, P.; Niu, H.; Du, Y.; Lin, T. A self-supported, flexible, binder-free pseudo-supercapacitor electrode material with high capacitance and cycling stability from hollow, capsular polypyrrole fibers. *J. Mater. Chem. A* **2015**, *3*, 16162–16167. [\[CrossRef\]](#)
46. Dubal, D.; Patil, S.; Kim, W.B.; Lokhande, C. Supercapacitors based on electrochemically deposited polypyrrole nanobricks. *Mater. Lett.* **2011**, *65*, 2628–2631. [\[CrossRef\]](#)
47. Shinde, S.S.; Gund, G.S.; Kumbhar, V.S.; Patil, B.H.; Lokhande, C.D. Novel chemical synthesis of polypyrrole thin film electrodes for supercapacitor application. *Eur. Polym. J.* **2013**, *49*, 3734–3739. [\[CrossRef\]](#)
48. Huang, Y.; Tao, J.; Meng, W.; Zhu, M.; Fu, Y.; Gao, Y.; Zhi, C. Super-high rate stretchable polypyrrole-based supercapacitors with excellent cycling stability. *Nano Energy* **2015**, *11*, 518–525. [\[CrossRef\]](#)
49. Gan, J.K.; Lim, Y.S.; Huang, N.M.; Lim, H.N. Hybrid silver nanoparticle/nanocluster-decorated polypyrrole for high-performance supercapacitors. *RSC Adv.* **2015**, *5*, 75442–75450. [\[CrossRef\]](#)
50. Iqbal, J.; Numan, A.; Ansari, M.O.; Jagadish, P.R.; Jafer, R.; Bashir, S.; Mohamad, S.; Ramesh, K.; Ramesh, S. Facile synthesis of ternary nanocomposite of polypyrrole incorporated with cobalt oxide and silver nanoparticles for high performance supercapattery. *Electrochim. Acta* **2020**, *348*, 136313. [\[CrossRef\]](#)
51. Guan, M.; Wang, Q.; Zhang, X.; Bao, J.; Gong, X.; Liu, Y. Two-Dimensional Transition Metal Oxide and Hydroxide-Based Hierarchical Architectures for Advanced Supercapacitor Materials. *Front. Chem.* **2020**, *8*, 390. [\[CrossRef\]](#)
52. Shi, F.; Li, L.; Wang, X.-L.; Gu, C.-D.; Tu, J.-P. Metal oxide/hydroxide-based materials for supercapacitors. *RSC Adv.* **2014**, *4*, 41910–41921. [\[CrossRef\]](#)
53. Cheng, J.; Zhang, J.; Liu, F. Recent development of metal hydroxides as electrode material of electrochemical capacitors. *RSC Adv.* **2014**, *4*, 38893–38917. [\[CrossRef\]](#)
54. Mao, Y.; Xie, J.; Liu, H.; Hu, W. Hierarchical core-shell Ag@Ni(OH)₂@PPy nanowire electrode for ultrahigh energy density asymmetric supercapacitor. *Chem. Eng. J.* **2021**, *405*, 126984. [\[CrossRef\]](#)
55. Shiri, H.M.; Ehsani, A.; Shayeh, J.S. Synthesis and highly efficient supercapacitor behavior of a novel poly pyrrole/ceramic oxide nanocomposite film. *RSC Adv.* **2015**, *5*, 91062–91068. [\[CrossRef\]](#)
56. Ariyanayagamkumarappa, D.; Zhitomirsky, I. Electropolymerization of polypyrrole films on stainless steel substrates for electrodes of electrochemical supercapacitors. *Synth. Met.* **2012**, *162*, 868–872. [\[CrossRef\]](#)
57. Zhu, Y.; Zhitomirsky, I. Influence of dopant structure and charge on supercapacitive behavior of polypyrrole electrodes with high mass loading. *Synth. Met.* **2013**, *185–186*, 126–132. [\[CrossRef\]](#)
58. Yang, X.; Xu, K.; Zou, R.; Hu, J. A Hybrid Electrode of Co₃O₄@PPy Core/Shell Nanosheet Arrays for High-Performance Supercapacitors. *Nano-Micro Lett.* **2016**, *8*, 143–150. [\[CrossRef\]](#) [\[PubMed\]](#)
59. Wei, H.; He, C.; Liu, J.; Gu, H.; Wang, Y.; Yan, X.; Guo, J.; Ding, D.; Shen, N.Z.; Wang, X.; et al. Electropolymerized polypyrrole nanocomposites with cobalt oxide coated on carbon paper for electrochemical energy storage. *Polymer* **2015**, *67*, 192–199. [\[CrossRef\]](#)
60. Wang, B.; He, X.; Li, H.; Liu, Q.; Wang, J.; Yu, L.; Yan, H.; Li, Z.; Wang, P. Optimizing the charge transfer process by designing Co₃O₄@PPy@MnO₂ ternary core-shell composite. *J. Mater. Chem. A* **2014**, *2*, 12968–12973. [\[CrossRef\]](#)
61. Ramesh, S.; Haldorai, Y.; Kim, H.S.; Kim, J.-H. A nanocrystalline Co₃O₄@polypyrrole/MWCNT hybrid nanocomposite for high performance electrochemical supercapacitors. *RSC Adv.* **2017**, *7*, 36833–36843. [\[CrossRef\]](#)
62. Chenga, Q.; Yangb, C.; Taoacd, K.; Hanacd, L. Inlaying ZIF-derived Co3S4 hollow nanocages on intertwined polypyrrole tubes conductive networks for high-performance supercapacitors. *Electrochim. Acta* **2020**, *341*, 136042. [\[CrossRef\]](#)
63. Guo, M.; Zhou, Y.; Sun, H.; Zhang, G.; Wang, Y. Interconnected polypyrrole nanostructure for high-performance all-solid-state flexible supercapacitor. *Electrochim. Acta* **2019**, *298*, 918–923. [\[CrossRef\]](#)
64. Xie, Y.; Zhou, Y. Enhanced electrochemical stability of CuCo bimetallic-coordinated polypyrrole. *Electrochim. Acta* **2018**, *290*, 419–428. [\[CrossRef\]](#)
65. Ates, M.; Serin, M.A.; Ekmen, I.; Ertas, Y.N. Supercapacitor behaviors of polyaniline/CuO, polypyrrole/CuO and PEDOT/CuO nanocomposites. *Polym. Bull.* **2015**, *72*, 2573–2589. [\[CrossRef\]](#)
66. Majumder, M.; Choudhary, R.B.; Thakur, A.K.; Karbhal, I. Impact of rare-earth metal oxide (Eu₂O₃) on the electrochemical properties of a polypyrrole/CuO polymeric composite for supercapacitor applications. *RSC Adv.* **2017**, *7*, 20037–20048. [\[CrossRef\]](#)
67. Peng, H.; Ma, G.; Sun, K.; Mu, J.; Wang, H.; Lei, Z. High-performance supercapacitor based on multi-structural CuS@polypyrrole composites prepared by in situ oxidative polymerization. *J. Mater. Chem. A* **2014**, *2*, 3303–3307. [\[CrossRef\]](#)
68. Peng, S.; Fan, L.; Wei, C.; Liu, X.; Zhang, H.; Xu, W.; Xu, J. Flexible polypyrrole/copper sulfide/bacterial cellulose nanofibrous composite membranes as supercapacitor electrodes. *Carbohydr. Polym.* **2017**, *157*, 344–352. [\[CrossRef\]](#)
69. Abdah, M.A.A.M.; Rahman, N.A.; Sulaiman, Y. Ternary functionalised carbon nanofibers/polypyrrole/manganese oxide as high specific energy electrode for supercapacitor. *Ceram. Int.* **2019**, *45*, 8433–8439. [\[CrossRef\]](#)
70. Yağan, A. Investigation of Polypyrrole-Based Iron Electrodes as Supercapacitors. *Int. J. Electrochem. Sci.* **2019**, *14*, 3978–3985. [\[CrossRef\]](#)
71. Wang, L.; Yang, H.; Liu, X.; Zeng, R.; Li, M.; Huang, Y.; Hu, X. Constructing Hierarchical Tectorum-like α-Fe₂O₃/PPy Nanoarrays on Carbon Cloth for Solid-State Asymmetric Supercapacitors. *Angew. Chem. Int. Ed.* **2016**, *56*, 1105–1110. [\[CrossRef\]](#) [\[PubMed\]](#)

72. Xu, C.; Santiago, A.R.P.; Rodríguez-Padrón, D.; Caballero, A.; Balu, A.M.; Romero, A.A.; Muñoz-Batista, M.J.; Luque, R. Controllable Design of Polypyrrole-Iron Oxide Nanocoral Architectures for Supercapacitors with Ultrahigh Cycling Stability. *ACS Appl. Energy Mater.* **2019**, *2*, 2161–2168. [\[CrossRef\]](#)
73. Sun, W.; Mo, Z. PPy/graphene nanosheets/rare earth ions: A new composite electrode material for supercapacitor. *Mater. Sci. Eng. B* **2013**, *178*, 527–532. [\[CrossRef\]](#)
74. Li, R.; Yang, Y.; Li, H.; Fu, R.; Tan, W.; Qin, Y.; Tao, Y.; Kong, Y. Design and synthesis of tungsten trioxide/polypyrrole/graphene using attapulgite as template for high-performance supercapacitors. *Electrochim. Acta* **2019**, *311*, 123–131. [\[CrossRef\]](#)
75. Vannathan, A.A.; Maity, S.; Kella, T.; Shee, D.; Das, P.P.; Mal, S.S. In situ vanadophosphomolybdate impregnated into conducting polypyrrole for supercapacitor. *Electrochim. Acta* **2020**, *364*, 137286. [\[CrossRef\]](#)
76. Gao, H.; Wang, X.; Wang, G.; Hao, C.; Zhou, S.; Huang, C. An urchin-like MgCo_2O_4 @PPy core-shell composite grown on Ni foam for a high-performance all-solid-state asymmetric supercapacitor. *Nanoscale* **2018**, *10*, 10190–10202. [\[CrossRef\]](#)
77. Wang, F.; Lv, X.; Zhang, L.; Zhang, H.; Zhu, Y.; Hu, Z.; Zhang, Y.; Ji, J.; Jiang, W. Construction of vertically aligned PPy nanosheets networks anchored on MnCo_2O_4 nanobelts for high-performance asymmetric supercapacitor. *J. Power Sources* **2018**, *393*, 169–176. [\[CrossRef\]](#)
78. Wang, H.; Song, Y.; Zhou, J.; Xu, X.; Hong, W.; Yan, J.; Xue, R.; Zhao, H.; Liu, Y.; Gao, J. High-performance supercapacitor materials based on polypyrrole composites embedded with core-sheath polypyrrole@ MnMoO_4 nanorods. *Electrochim. Acta* **2016**, *212*, 775–783. [\[CrossRef\]](#)
79. Huang, J.; Qian, X.; An, X.; Li, X.; Guan, J. Double in situ fabrication of PPy@ MnMoO_4 /cellulose fibers flexible electrodes with high electrochemical performance for supercapacitor applications. *Cellulose* **2020**, *27*, 5829–5843. [\[CrossRef\]](#)
80. Yao, W.; Zhou, H.; Lu, Y. Synthesis and property of novel MnO_2 @polypyrrole coaxial nanotubes as electrode material for supercapacitors. *J. Power Sources* **2013**, *241*, 359–366. [\[CrossRef\]](#)
81. Wang, J.-G.; Yang, Y.; Huang, Z.-H.; Kang, F. MnO_2 /polypyrrole nanotubular composites: Reactive template synthesis, characterization and application as superior electrode materials for high-performance supercapacitors. *Electrochim. Acta* **2014**, *130*, 642–649. [\[CrossRef\]](#)
82. Bahloul, A.; Nessark, B.; Briot, E.; Groult, H.; Mauger, A.; Zaghib, K.; Julien, C. Polypyrrole-covered MnO_2 as electrode material for supercapacitor. *J. Power Sources* **2013**, *240*, 267–272. [\[CrossRef\]](#)
83. Wang, J.-G.; Wei, B.; Kang, F. Facile synthesis of hierarchical conducting polypyrrole nanostructures via a reactive template of MnO_2 and their application in supercapacitors. *RSC Adv.* **2014**, *4*, 199–202. [\[CrossRef\]](#)
84. Yuan, L.; Wan, C.; Zhao, L. Facial In-situ Synthesis of MnO_2 /PPy Composite for Supercapacitor. *Int. J. Electrochem. Sci.* **2015**, *10*, 9456–9465.
85. Fan, X.; Wang, X.; Li, G.; Yu, A.; Chen, Z. High-performance flexible electrode based on electrodeposition of polypyrrole/ MnO_2 on carbon cloth for supercapacitors. *J. Power Sources* **2016**, *326*, 357–364. [\[CrossRef\]](#)
86. Liang, F.; Liu, Z.; Liu, Y. Enhanced electrochemical properties of MnO_2 /PPy nanocomposites by miniemulsion polymerization. *J. Mater. Sci. Mater. Electron.* **2017**, *28*, 10603–10610. [\[CrossRef\]](#)
87. Li, J.; Que, T.; Huang, J. Synthesis and characterization of a novel tube-in-tube nanostructured PPy/ MnO_2 /CNTs composite for supercapacitor. *Mater. Res. Bull.* **2013**, *48*, 747–751. [\[CrossRef\]](#)
88. He, M.; Zheng, Y.; Du, Q. Three-dimensional polypyrrole/ MnO_2 composite networks deposited on graphite felt as free-standing electrode for supercapacitors. *Mater. Lett.* **2013**, *104*, 48–52. [\[CrossRef\]](#)
89. Dong, Z.H.; Wei, Y.L.; Shi, W.; Zhang, G.A. Characterisation of doped polypyrrole/manganese oxide nanocomposite for supercapacitor electrodes. *Mater. Chem. Phys.* **2011**, *131*, 529–534. [\[CrossRef\]](#)
90. Zhang, X.; Zeng, X.; Yang, M.; Qi, Y. Investigation of a Branchlike MoO_3 /Polypyrrole Hybrid with Enhanced Electrochemical Performance Used as an Electrode in Supercapacitors. *ACS Appl. Mater. Interfaces* **2013**, *6*, 1125–1130. [\[CrossRef\]](#) [\[PubMed\]](#)
91. Ma, G.; Peng, H.; Mu, J.; Huang, H.; Zhou, X.; Lei, Z. In situ intercalative polymerization of pyrrole in graphene analogue of MoS_2 as advanced electrode material in supercapacitor. *J. Power Sources* **2013**, *229*, 72–78. [\[CrossRef\]](#)
92. Chen, Y.; Ma, W.; Cai, K.; Yang, X.; Huang, C. In Situ Growth of Polypyrrole onto Three-Dimensional Tubular MoS_2 as an Advanced Negative Electrode Material for Supercapacitor. *Electrochim. Acta* **2017**, *246*, 615–624. [\[CrossRef\]](#)
93. Karaca, E.; Gökçen, D.; Pekmez, N.Ö.; Pekmez, K. Electrochemical synthesis of PPy composites with nanostructured MnOx , CoOx , NiOx , and FeOx in acetonitrile for supercapacitor applications. *Electrochim. Acta* **2019**, *305*, 502–513. [\[CrossRef\]](#)
94. Na Choi, B.; Chun, W.W.; Qian, A.; Lee, S.J.; Chung, C.-H. Dendritic Ni(Cu)-polypyrrole hybrid films for a pseudo-capacitor. *Nanoscale* **2015**, *7*, 18561–18569. [\[CrossRef\]](#) [\[PubMed\]](#)
95. Zhang, J.; Liu, Y.; Guan, H.; Zhao, Y.; Zhang, B. Decoration of nickel hydroxide nanoparticles onto polypyrrole nanotubes with enhanced electrochemical performance for supercapacitors. *J. Alloy. Compd.* **2017**, *721*, 731–740. [\[CrossRef\]](#)
96. Brzózka, A.; Fic, K.; Bogusz, J.; Brudzisz, A.M.; Marzec, M.M.; Gajewska, M.; Sulka, G.D. Polypyrrole-Nickel Hydroxide Hybrid Nanowires as Future Materials for Energy Storage. *Nanomaterials* **2019**, *9*, 307. [\[CrossRef\]](#)
97. Wang, Y.; Chen, Y.; Liu, Y.; Liu, W.; Zhao, P.; Li, Y.; Dong, Y.; Wang, H.; Yang, J. Urchin-like $\text{Ni}_{1/3}\text{Co}_{2/3}(\text{CO}_3)_{0.5}\text{OH}\cdot 0.11\text{H}_2\text{O}$ anchoring on polypyrrole nanotubes for supercapacitor electrodes. *Electrochim. Acta* **2019**, *295*, 989–996. [\[CrossRef\]](#)
98. Liu, S.; Chen, Y.; Ren, J.; Wang, Y.; Wei, W. An effective interaction in polypyrrole/nickel phosphide (PPy/ Ni_2P) for high-performance supercapacitor. *J. Solid State Electrochem.* **2019**, *23*, 3409–3418. [\[CrossRef\]](#)

99. Wu, X.; Lian, M.; Wang, Q. A high-performance asymmetric supercapacitors based on hydrogen bonding nanoflower-like polypyrrole and NiCo(OH)₂ electrode materials. *Electrochim. Acta* **2019**, *295*, 655–661. [\[CrossRef\]](#)
100. Chen, T.; Fan, Y.; Wang, G.; Zhang, J.; Chuo, H.; Yang, R. Rationally Designed Carbon Fiber@NiCo₂O₄@Polypyrrole Core–Shell Nanowire Array for High-Performance Supercapacitor Electrodes. *Nano* **2016**, *11*, 1650015. [\[CrossRef\]](#)
101. Zhang, J.; Guan, H.; Liu, Y.; Zhao, Y.; Zhang, B. Hierarchical polypyrrole nanotubes@NiCo₂S₄ nanosheets core-shell composites with improved electrochemical performance as supercapacitors. *Electrochim. Acta* **2017**, *258*, 182–191. [\[CrossRef\]](#)
102. Zheng, Y.; Xu, J.; Yang, X.; Zhang, Y.; Shang, Y.; Hu, X. Decoration NiCo₂S₄ nanoflakes onto Ppy nanotubes as core-shell heterostructure material for high-performance asymmetric supercapacitor. *Chem. Eng. J.* **2018**, *333*, 111–121. [\[CrossRef\]](#)
103. Yan, M.; Yao, Y.; Wen, J.; Long, L.; Kong, M.; Zhang, G.; Liao, X.; Yin, G.; Huang, Z. Construction of a Hierarchical NiCo₂S₄@PPy Core–Shell Heterostructure Nanotube Array on Ni Foam for a High-Performance Asymmetric Supercapacitor. *ACS Appl. Mater. Interfaces* **2016**, *8*, 24525–24535. [\[CrossRef\]](#) [\[PubMed\]](#)
104. Scindia, S.S.; Kamble, R.B.; Kher, J.A. Nickel ferrite/polypyrrole core-shell composite as an efficient electrode material for high-performance supercapacitor. *AIP Adv.* **2019**, *9*, 055218. [\[CrossRef\]](#)
105. Yuan, Y.; Zhou, J.; Rafiq, M.I.; Dai, S.; Tang, J.; Tang, W. Growth of Ni Mn layered double hydroxide and polypyrrole on bacterial cellulose nanofibers for efficient supercapacitors. *Electrochim. Acta* **2019**, *295*, 82–91. [\[CrossRef\]](#)
106. Zhang, Y.; Du, D.; Li, X.; Sun, H.; Li, L.; Bai, P.; Xing, W.; Xue, Q.; Yan, Z. Electrostatic Self-Assembly of Sandwich-Like CoAl-LDH/Polypyrrole/Graphene Nanocomposites with Enhanced Capacitive Performance. *ACS Appl. Mater. Interfaces* **2017**, *9*, 31699–31709. [\[CrossRef\]](#)
107. Shao, M.; Li, Z.; Zhang, R.; Ning, F.; Wei, M.; Evans, D.G.; Duan, X. Hierarchical Conducting Polymer@Clay Core-Shell Arrays for Flexible All-Solid-State Supercapacitor Devices. *Small* **2015**, *11*, 3530–3538. [\[CrossRef\]](#)
108. Wang, B.; Li, W.; Liu, Z.; Duan, Y.; Zhao, B.; Wang, Y.; Liu, J. Incorporating Ni-MOF structure with polypyrrole: Enhanced capacitive behavior as electrode material for supercapacitor. *RSC Adv.* **2020**, *10*, 12129–12134. [\[CrossRef\]](#)
109. Li, X.; Zhang, Y.; Xing, W.; Li, L.; Xue, Q.; Yan, Z. Sandwich-like graphene/polypyrrole/layered double hydroxide nanowires for high-performance supercapacitors. *J. Power Sources* **2016**, *331*, 67–75. [\[CrossRef\]](#)
110. Yadav, H.M.; Ramesh, S.; Kumar, K.A.; Shinde, S.; Sandhu, S.; Sivasamy, A.; Shrestha, N.K.; Kim, H.S.; Kim, H.-S.; Bathula, C. Impact of polypyrrole incorporation on nickel oxide@multi walled carbon nanotube composite for application in supercapacitors. *Polym. Test.* **2020**, *89*, 106727. [\[CrossRef\]](#)
111. Vijeth, H.; Ashokkumar, S.; Yesappa, L.; Vandana, M.; Devendrappa, H. Hybrid core-shell nanostructure made of chitosan incorporated polypyrrole nanotubes decorated with NiO for all-solid-state symmetric supercapacitor application. *Electrochim. Acta* **2020**, *354*, 136651. [\[CrossRef\]](#)
112. Peng, S.; Fan, L.; Wei, C.; Bao, H.; Zhang, H.; Xu, W.; Xu, J. Polypyrrole/nickel sulfide/bacterial cellulose nanofibrous composite membranes for flexible supercapacitor electrodes. *Cellulose* **2016**, *23*, 2639–2651. [\[CrossRef\]](#)
113. Sarmah, D.; Kumar, A. Layer-by-layer self-assembly of ternary MoS₂-rGO@PPyNTs nanocomposites for high performance supercapacitor electrode. *Synth. Met.* **2018**, *243*, 75–89. [\[CrossRef\]](#)
114. Sarmah, D.; Kumar, A. Ion beam modified molybdenum disulfide-reduced graphene oxide/ polypyrrole nanotubes ternary nanocomposite for hybrid supercapacitor electrode. *Electrochim. Acta* **2019**, *312*, 392–410. [\[CrossRef\]](#)
115. Eeu, Y.C.; Lim, H.N.; Lim, Y.S.; Zakarya, S.A.; Huang, N.M. Electrodeposition of Polypyrrole/Reduced Graphene Oxide/Iron Oxide Nanocomposite as Supercapacitor Electrode Material. *J. Nanomater.* **2013**, *2013*, 1–6. [\[CrossRef\]](#)
116. Lee, H.; Cho, M.S.; Kim, I.H.; Nam, J.D.; Lee, Y. RuOx/polypyrrole nanocomposite electrode for electrochemical capacitors. *Synth. Met.* **2010**, *160*, 1055–1059. [\[CrossRef\]](#)
117. Liu, P.; Wang, Y.; Wang, X.; Yang, C.; Yi, Y. Polypyrrole-coated samarium oxide nanobelts: Fabrication, characterization, and application in supercapacitors. *J. Nanoparticle Res.* **2012**, *14*, 1232. [\[CrossRef\]](#)
118. De Oliveira, A.H.P.; de Oliveira, H.P. Carbon nanotube/ polypyrrole nanofibers core-shell composites decorated with titanium dioxide nanoparticles for supercapacitor electrodes. *J. Power Sources* **2014**, *268*, 45–49. [\[CrossRef\]](#)
119. Kim, M.S.; Park, J.H. Polypyrrole/titanium oxide nanotube arrays composites as an active material for supercapacitors. *J. Nanosci. Nanotechnol.* **2011**, *11*, 4522–4526. [\[CrossRef\]](#) [\[PubMed\]](#)
120. Bai, M.-H.; Bian, L.-J.; Song, Y.; Liu, X.-X. Electrochemical Codeposition of Vanadium Oxide and Polypyrrole for High-Performance Supercapacitor with High Working Voltage. *ACS Appl. Mater. Interfaces* **2014**, *6*, 12656–12664. [\[CrossRef\]](#)
121. Chen, T.; Fan, Y.; Wang, G.; Yang, Q.; Yang, R. Rationally designed hierarchical ZnCo₂O₄/polypyrrole nanostructures for high-performance supercapacitor electrodes. *RSC Adv.* **2015**, *5*, 74523–74530. [\[CrossRef\]](#)
122. Sidhu, N.K.; Rastogi, A.C. Vertically aligned ZnO nanorod core-polypyrrole conducting polymer sheath and nanotube arrays for electrochemical supercapacitor energy storage. *Nanoscale Res. Lett.* **2014**, *9*, 453. [\[CrossRef\]](#)
123. Elahi, H.; Munir, K.; Eugeni, M.; Atek, S.; Gaudenzi, P. Energy Harvesting towards Self-Powered IoT Devices. *Energies* **2020**, *13*, 5528. [\[CrossRef\]](#)